Solvent-dependent dynamics of hydrogen bonding structure 5-(methylthio)-1, 3, 4-thiadiazole-2(3H)-thione as determined by Raman spectroscopy and theoretical calculation

Sumei Pang [a], Yanying Zhao [a,b,*], Xin Liu [a], Jiadan Xue [a,b], Xuming Zheng [a,b,*]

[a] Department of Chemistry, Zhejiang Sci-Tech University, Hangzhou 310018, China
[b] State Key Laboratory of Advanced Textiles Materials and Manufacture Technology, Ministry of Education(MOE), Zhejiang Sci-Tech University, Hangzhou 310018, China

ARTICLE INFO

ABSTRACT

The vibration spectra of 5-(methylthio)-1,3,4-thiadiazole-2($3H$)-thione (MTTN) in acetonitrile (CH_3CN), methanol (CH_3OH) and water (H_2O) solvents were collected and evaluated via deuterium isotopic substitution Raman spectroscopic experiments. These experiments were combined with the quantum chemical theoretical calculations using the PCM solvent model and normal mode analysis. The results confirmed that the MTTN in CH_3CN, CH_3OH and H_2O have hydrogen bonding (H-bonding) MTTN(solvent)$_n$ clusters that produce significantly different Raman intensity patterns in different solvents. Combined with the normal Raman assignment, most resonance Raman spectra were assigned to the vibration modes of the H-bonding MTTN(CH_3CN), MTTN(CH_3OH)$_3$ and MTTN(H_2O)$_3$ clusters in CH_3CN, CH_3OH and H_2O. The theoretically-predicted frequencies and intensities in different surrounding environments enabled reliable assignments of Raman bands. The intermolecular > NH···O O and >NH···N H-bonding interactions are key constituents of stable thione structures in MTTN. This underlines the significant structural differences of MTTN in CH_3CN, CH_3OH and H_2O. H-bonding perturbation of MTTN reveal important insights about the intermolecular excited state proton transfer (ESPT) reaction mechanisms in the Franck-Condon region structural dynamics of the thione → thiol tautomer in CH_3OH and H_2O.

© 2016 Elsevier B.V. All rights reserved.

1. Introduction

Many weak intermolecular interactions such as van der Waals, electrostatic and hydrogen-bonding interactions between solute and solvent molecules can usually control the possible conformations of solute molecules in solvents and correspond to energy minima on an intricate potential energy surface [1–3]. Of these interactions, understanding the thermodynamics and dynamics of hydrogen-bonding plays a fundamental role in the physical chemistry, biology, materials and earth and planetary sciences [4–6]. The in-solution competition of the conformations with intra- or inter-molecular hydrogen bonding (H-bonding) for small organic molecules has been reviewed. The balance of the increased internal energy and the stabilizing effect of the solute-solvent interactions regulate the new conformer composition in the liquid phase. An intramolecular H-bonding is possible in gas, while in a polar protic solution, the intramolecular H-bonding may be disrupted in favor of two solute-solvent intermolecular H-bondings [7]. Infrared (IR) and Raman spectroscopy can provide quantitative information on H-bonding systems [8–13]. Since the initial observation of hydrogen-bond scalar couplings (HBCs) for N—H···N H-bondings in Watson–

Crick base pairs of nucleic acids, there have been only a few neutron diffraction and ultra-high-resolution X-ray techniques to study the positions of hydrogen atoms. These were determined within the H-bonding without the use of fixed standard geometries [14–16]. The X-ray and neutron diffraction methods made invaluable contributions to the present knowledge of H-bondings in terms of the exact positions of donor and acceptor groups. Raman spectroscopy is also a compelling tool to characterize and clarify the structural details of the solute-solvent molecules except for the fluorescence emission disturbance.

In 5-(methylthio)-1,3,4-thiadiazole-2($3H$)-thione molecule, the thiocarbonyl C=S group is attached directly to the heterocyclic ring. It was placed in a position with respect to the NH group that was regarded as one of the thioamide derivatives. In the MTTN molecular structures, analogous thione-thiol photoreactions were found for simple thioamides such as thiourea [17] and thioacetamide [18]. Considering the enormous biological and medical applications of the 2, 5-disubstituted 1, 3, 4-thiadiazole derivatives [19–21], tautomerism of monomeric MTTN was studied using a matrix-isolation technique [22]. Only the thione tautomeric forms were observed after deposition of the Ar matrices. This was after UV irradiation, and the most stable thione form was transformed into the corresponding thiol tautomers via an intramolecular proton transfer reaction. Combining the Møller–Plesset perturbation theory of the second order(MP2) and Becke, three-parameter, Lee-Yang-

---

Parr(B3LYP) calculations, the Raman spectra, infrared spectra and Nuclear Magnetic Resonance(NMR) measurements clearly favored the thione tautomeric form with *cis* configuration of CH_3S moiety to the S-atom of the thiadiazole ring [23]. Subsequently, Chowdhury and coworkers reported the Fourier Transform Infrared spectroscopy(FTIR), Normal Raman spectra(NRS) and surface-enhanced Raman scatting(SERS) of MTTN on the nanocolloidal silver surface. They used Density functional theory(DFT) vibrational calculations to show that the surface selection rule orientated both thione and thiol forms of MTTN in acetonitrile solvent due to Albrecht's "A" and Herzberg-Teller (HT) charge transfer (CT) contribution. This produced selective enhancement of Raman bands observed at ~600, 1070, 1350 and 1390 cm^{-1} [24].

Here, MTTN was further investigated in acetonitrile(CH_3CN), methanol(CH_3OH), and water(H_2O) to probe the interactions between the MTTN and solvent molecules by non-resonance and resonance Raman spectroscopy. Deuterium isotopic substituted Raman experiments confirmed that the solute-solvent intermolecular H-bonding could be formed in MTTN with CH_3CN, CH_3OH, and H_2O in the corresponding solvents. DFT calculations concluded that the intermolecular >NH⋯O and >NH⋯N H-bonding play a vital role on the stability of the thiocarbonyl isomer of MTTN. The resonance Raman spectra observed in different solvent environments were assigned to MTTN-associated solvent molecules. The excited state structural dynamics and proton transfer of MTTN in CH_3CN, CH_3OH, and H_2O were also preliminarily explored.

2. Experimental and Theoretical Details

5-(Methylthio)-1, 3, 4-thiadiazole-2(3H)-thione (MTTN, 98% purity, China), deuterium oxide (D_2O, 99.8 atom% D) and methanol-d4 (CD_3OD, 99.8 atom% D) were purchased from J&K Chemical Company and used without purification. Concentrations of approximately 2.0×10^{-3}-5.0×10^{-3} mol·L^{-1} were prepared using HPLC grade solvents of acetonitrile (99.9%, Tedia, USA), methanol (99.9%, Spectrum, USA) and de-ionized water.

The Fourier transform (FT)-Raman (1064 nm) spectra were obtained using a FT-Raman spectrometer (Thermo Nicolet 960, Thermo Fisher Nicolet, USA) with 2 cm^{-1} resolution. The visible excitation laser line (488 nm) was produced with a CVI MellesGriot argon ion laser (543-AP-A01). A backscattering geometry was employed for collection of the Raman scattered light by reflective optics that imaged the light onto a liquid nitrogen cooled CCD mounted on the exit of the spectrograph. Raman backscattering spectra were recorded using a 20× objective lens with a ~2 cm^{-1} resolution TriVista Spectrometer System equipped with a research-grade SPAHL-20 microscope. The 918 cm^{-1}, 1376 cm^{-1}, 2249 cm^{-1} and 2942 cm^{-1} bands of CH_3CN [25] were used for calibration. The resonance Raman spectra (309.1 and 319.9 nm) were obtained by the resonance Raman experimental apparatus. This has been described elsewhere [26–29]. The harmonics of a nanosecond Nd:YAG laser and their hydrogen Raman shifted laser lines were employed to generate the 319.9 nm excitation wavelengths that were utilized in the resonance Raman experiments. The excitation laser beam used a ~100 J pulse energy, which was loosely focused on a 0.5–1.0 mm diameter spot size of flowing sample. The Raman shifts of the resonance Raman spectra were calibrated with the known vibrational frequencies of solvent Raman bands (CH_3CN, CH_3OH, and H_2O).

Quantum chemical calculations were performed using the Gaussian 09 program [30]. The geometry optimized calculations, Raman vibrational frequencies and polarized continuum overlapping spheres model (PCM) are performed at the level of density functional theory (DFT) with the hybrid BVP86 and second-order perturbation MP2 methods [31–33]. The 6-31G(d) and 6-311++G(d, p) basis sets were used for all atoms [34–36]. The bonding characteristics were analyzed using natural bond orbital (NBO) theory, which was achieved with the NBO 3.1 package as implemented in Gaussian 09 [37]. The normal mode analysis of used the VEDA program coded by Michal H. Jamróz [38].

3. Results and Discussion

Fig. 1 confirms the intensity pattern of the experimental 1064, 488 and 319.9 nm Raman spectra in the 400–1600 cm^{-1} region for MTTN in CH_3CN. Several strong bands at ~1491, 1441, 1051 and 648 cm^{-1} exhibit identical intensity patterns with 1064, 488 and 319.9 nm excitation wavelengths in CH_3CN solvent. The normal 488, and 319.9 nm resonance Raman spectra are shown in Figs. 2 and 3 in the selected regions in CH_3CN, CH_3OH, and H_2O. The intensity pattern of 488 and 319.9 nm resonance Raman spectra of MTTN in H_2O is analogous to those in CH_3OH. Some vibrational bands of the 319.9 nm resonance Raman spectra of MTTN in CH_3CN differ from those in CH_3OH and H_2O, as shown in Fig. 2. The strong bands at 549, 661, 1055 and 1453 cm^{-1} in H_2O are relative to 546, 650, 1050 and 1453 cm^{-1} in CH_3OH. In the 1400–1600 cm^{-1} region, there is an intense band at 1453 cm^{-1} in H_2O and CH_3OH. Two strong bands are observed at 1491 and 1441 cm^{-1} in CH_3CN. For the band at 1491 cm^{-1} in CH_3CN, it becomes very weak at 1495 cm^{-1} in CH_3OH and even disappears in H_2O. A moderate intensity band at 1400 cm^{-1} in H_2O is not observed in CH_3OH and CH_3CN. The 648 cm^{-1} band in CH_3CN is 13 cm^{-1} blue-shifts observed at 661 cm^{-1} in H_2O. In contrast, the stronger intensity pattern of 488 nm Raman spectra of MTTN in CH_3OH is somewhat similar to those in H_2O, but it is also completely different from CH_3CN, as shown in Fig. 3.

To clarify the band shifts and the peak disappearance and emergence in different solvents, the 488 nm Raman spectroscopic experiments are repeated with isotopic substituted CD_3OD and D_2O solvent samples (Figs. 4 and 5). The observed frequencies in CD_3OD and D_2O are also listed in Table 1. As shown in Fig. 4, the bands at 1051 and 1275 cm^{-1} in CH_3OH are red-shifted to 1045 and 1348 cm^{-1} in CD_3OD, respectively. However, the 1106 and 1454 cm^{-1} bands in CH_3OH are blue-shifted by 13 and 14 cm^{-1} relative to the bands at 1119 and 1468 cm^{-1} in CD_3OD, respectively. The weak band at 1497 cm^{-1} is difficult to observe in CD_3OD due to low intensity.

In addition to these bands with large deuterium shifts, the bands at 650 and 701 cm^{-1} show less than a 2 cm^{-1} deuterium shift. On the contrary, Fig. 5 shows that the 648 cm^{-1} band in CH_3CN is blue-shifted by 661 cm^{-1} in H_2O and then red-shifted back to 648 cm^{-1} in D_2O. Strong residual bands move from 1055, 1400 and 1453 cm^{-1} in H_2O to 1047, 1396 and 1461 cm^{-1} in D_2O. On the basis of previous assignments [22–24], the bands at 545, 648, 701, 1051 and 1441 and 1491 cm^{-1} in CH_3CN were assigned to (S=)C-S stretching + C—S(CH_3) stretching + (S=)C—N—H out of the ring stretching, (S=)C—S—C(—SCH_3) in the ring stretching + N—N—C(=S) + N—N—H in-plane bending, C=S stretching
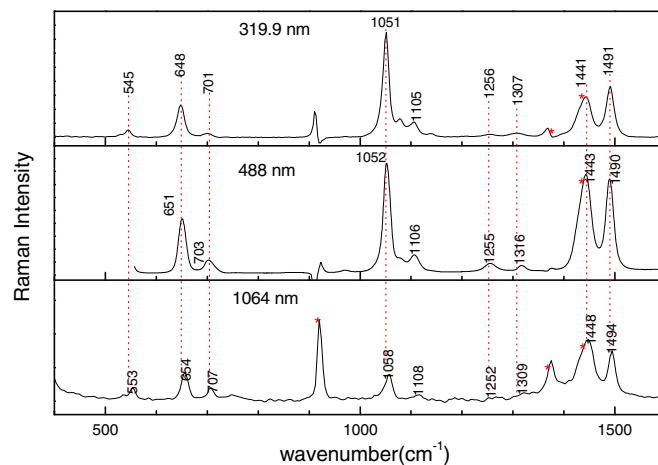

Fig. 1. The Raman spectra in the 400–1600 cm^{-1} region of MTTN with 1064, 488 and 319.9 nm excitation wavelengths in CH_3CN solvent. Asterisks label parts of the spectrum where solvent subtraction artifacts are present.